ELSEVIER

Quaternary Science Reviews 25 (2006) 1247–1263

QSR

Lateglacial and Holocene sediment sources and transport patterns in the Skagerrak interpreted from high-resolution magnetic properties and grain size data

Richard Gyllencreutz[a,*], Catherine Kissel[b]

[a]*Department of Geology and Geochemistry, Stockholm University, SE-10691 Stockholm, Sweden*
[b]*Laboratoire des Sciences du Climat et de l'Environnement, CEA/CNRS, Gif-sur-Yvette, Avenue de la Terrasse, Bat 12, 91198 Gif-sur-Yvette Cedex, France*

Received 31 January 2005; accepted 3 November 2005

Abstract

Lateglacial and Holocene changes in circulation, sedimentation and provenance in north-eastern Skagerrak were studied using high-resolution mineral magnetic and grain size data from the 32-m-long IMAGES core MD99-2286. Ages are given in calibrated thousand years BP ('cal. kyr'). Between 12 and 11.3 cal. kyr, a calving ice front occupied the Oslo Fjord, and sedimentation was strongly influenced by meltwater carrying re-deposited glacial sediments from southern Norway and western Sweden. Between 11.3 and 10.3 cal. kyr, sedimentation was dominated by re-deposited glacial sediments transported by meltwater outflow across south-central Sweden. After the Otteid-Stenselva outlet was closed at 10.3 cal. kyr, glacial marine sedimentation changed to normal marine sedimentation. At 8.5 cal. kyr, a hydrographic shift, marking the onset of modern circulation in the Skagerrak–Kattegat, occurred as a result of increased Atlantic inflow, transgression of former land areas, and opening of the English Channel and the Danish Straits. After 8.5 cal. kyr, sedimentation was governed by input from the Atlantic Ocean and the North Sea, with varying contributions from the South Jutland Current, Baltic Current, and currents along the coasts of western Sweden and southern Norway. From 0.9 cal. kyr until present, the sedimentation was totally dominated by southern North Sea and Atlantic Ocean sources.

1. Introduction

The Skagerrak is the major sink for fine-grained sediment in the North Sea region. The circulation and subsequent sedimentation in the Skagerrak is mainly driven by the North Atlantic Current, with important contributions from the Jutland Current, and minor contributions from Baltic Sea outflow and continental runoff (Longva and Thorsnes, 1997). In the north-eastern Skagerrak, the cyclonic circulation of mixed water masses with a large sediment load is greatly slowed down, causing deposition of suspended material at high relative rates (Bøe et al., 1996).

The sediment sequences in the Skagerrak preserve records of climatic and oceanographic changes of the North Sea region including adjacent land areas, and have been the focus of many paleoceanographic studies during the last decades (e.g., Fält, 1982; Stabell and Thiede, 1985; Nordberg, 1991; Bergsten, 1994; Conradsen and Heier-Nielsen, 1995; Hass, 1996; Jiang et al., 1997). Previous studies of cores from the Norwegian Channel and the Skagerrak–Kattegat area have shown marked changes in sedimentation (Bergsten, 1989, 1991, 1994) during the period of Baltic outflow through south central Sweden at ca 11.3–10.3 cal. kyr (Björck, 1995). Distinct hydrographic shifts in the Skagerrak–Kattegat have been suggested at ca 9.0–8.0 cal. kyr and 6.2–4.0 cal. kyr (Nordberg, 1991; Conradsen and Heier-Nielsen, 1995; Jiang et al., 1997; Klitgaard-Kristensen et al., 2001). However, discrepancies in the dating of these changes and the use of different time resolutions of the studied cores have resulted in debate of the timing and extent of the observed shifts (Nordberg,

*Corresponding author. Current address: Department of Earth Science, University of Bergen, Allégaten 41, No-5007 Bergen, Norway.
Tel.: +47 555 83537; fax: +47 555 83660.
E-mail address: richard.gyllencreutz@geo.uib.no (R. Gyllencreutz).

0277-3791/$ - see front matter © 2005 Elsevier Ltd. All rights reserved.
doi:10.1016/j.quascirev.2005.11.002

1991; Conradsen, 1995; Conradsen and Heier-Nielsen, 1995; Jiang et al., 1997). The sedimentation in the Skagerrak was comprehensively reviewed by van Weering et al. (1993), and has been the focus of several special volumes (Stabell and Thiede, 1985; Liebezeit et al., 1993; Bøe and Thorsnes, 1996; Longva and Thorsnes, 1997). It can be concluded from these efforts that there are a limited number of high-resolution studies (decadal or better) of long Skagerrak cores having accurate chronostratigraphic control.

Studies focused on transport mechanisms and source areas have shown that the sediments in the north-eastern Skagerrak are mainly deposited from suspension, consisting of a mixture of material derived from the North Sea/Atlantic Ocean, Scandinavia/Baltic Sea and reworked material from mainly the southern North Sea (van Weering, 1981; Eisma and Kalf, 1987; Eisma and Irion, 1988; Kuijpers et al., 1993; van Weering et al., 1993; Rodhe and Holt, 1996; Longva and Thorsnes, 1997). The spatial variation in mineral magnetic properties has been investigated in a study of 74 surface samples from the Norwegian part of the Skagerrak (Lepland and Stevens, 1996). As a result of this study, two major provinces reflecting different source areas for the northern Skagerrak sediments were defined: a "Norwegian" mineral population distributed along the Norwegian coast and in the north-eastern Skagerrak, and a "Danish" population occupying the central part of the Skagerrak.

Previous magnetic investigations of cores from the Skagerrak have focused on dating and stratigraphic correlation, and are limited to the Solberga-2 core (Abrahamsen, 1982) and the GIK 15530-4 core (Schoenharting, 1985). The application of mineral magnetic methods to problems related to transport, deposition and transformation of magnetic grains in sedimentary environments has been proven to be useful for paleo-environmental interpretation in various depositional settings (Robinson et al., 1995; Lepland and Stevens, 1996; Colin et al., 1998; Kissel et al., 1999).

The present study is aimed to investigate sedimentation and source area variability throughout the Holocene on a sub-centennial to sub-decadal resolution, using mineral magnetic properties and detailed grain size analysis in the 32-m-long and AMS 14C-dated sediment core MD99-2286, recovered during the IMAGES-GINNA cruise on board the R/V *Marion Dufresne* from a location at the border between the two source-area populations in the north-eastern Skagerrak.

2. Oceanographic and sedimentary setting

The Skagerrak forms a sedimentary basin in the inner end of the Norwegian Trench (Fig. 1), and is bordered by the coasts of Denmark, Sweden and Norway. It is the deepest part of the otherwise relatively shallow North Sea, with water depths exceeding 700 m. The present large-scale circulation in the Skagerrak (Fig. 1) has been described by

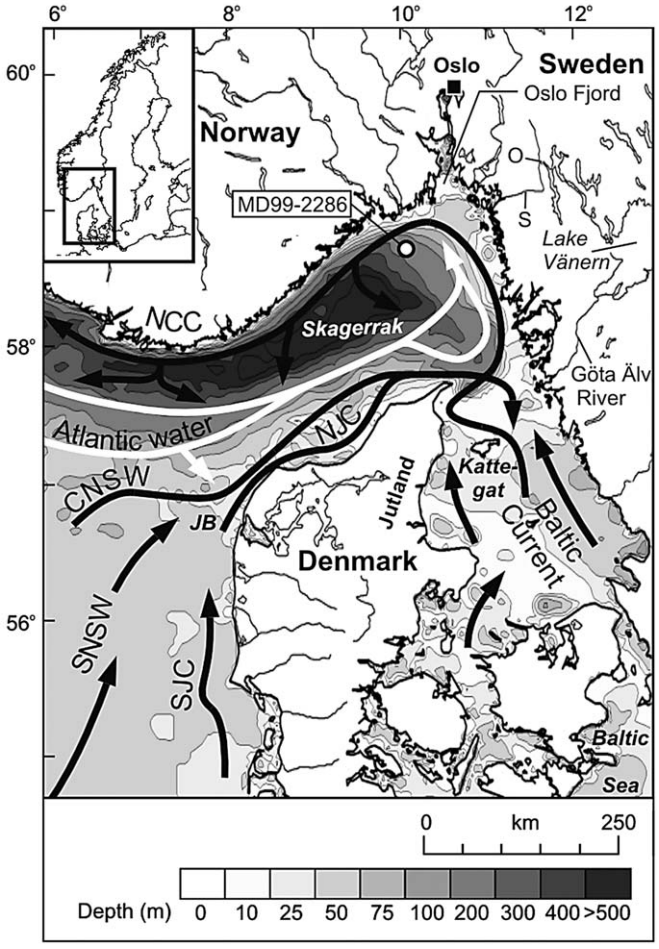

Fig. 1. General ocean circulation (arrows) and bathymetry in the Skagerrak and the eastern North Sea. White arrows mark the part of Atlantic water which flows more or less directly into the Skagerrak. NJC = North Jutland Current, SJC = South Jutland Current (NJC + SJC = Jutland Current), SNSW = South North Sea Water, CNSW = Central North Sea Water, and NCC = Norwegian Coastal Current, O = Otteid strait, S = Stenselva strait, and JB = Jutland Bank. The location of core MD99-2286 is marked with a circle. Current pattern modified from Longva and Thorsnes (1997). Bathymetry from the ETOPO2 database (Smith and Sandwell, 1997).

Svansson (1975), Rodhe (1987, 1996, 1998) and reviewed by Otto et al. (1990). The circulation and subsequent sedimentation in the Skagerrak is mainly governed by the North Atlantic Current, through water entering the North Sea between Scotland and Norway in the north and via the English Channel in the southwest. English Channel water and relatively small amounts of low salinity river outflow mixes with Southern North Sea Water, and continues as the highly variable Jutland Current along the Danish west coast towards the Skagerrak (Longva and Thorsnes, 1997). The Jutland Current mixes with the Central North Sea Water and with relatively fresh and cold outflow waters from the Baltic Sea as it moves further to the north-east. This mixed current makes a counter-clockwise turn in the northeastern end of the Skagerrak, forming the Norwegian Coastal Current. This current follows the Norwegian

trench to the southwest, where it exits the Skagerrak and continues north along the coast of Norway. In the course of the cyclonic turn in the eastern Skagerrak, the water depth increases and the current speed is reduced beyond the limit where the intensity of turbulence can support a steady concentration of suspended matter (Rodhe and Holt, 1996). Because of this, fine-grained sediments are deposited at a high relative rate, up to 1 cm/year, in the northeastern and central parts of the Skagerrak (van Weering, 1982; Bøe et al., 1996).

The present-day Jutland Current consists of two branches, the North Jutland Current (NJC) and the South Jutland Current (SJC) (Nordberg, 1991). The NJC transports large volumes of Atlantic Water with a low concentration of suspended sediment along the southern flank of the Norwegian Trench, and accounts for about 90% of the inflow to the Skagerrak (Longva and Thorsnes, 1997). The SJC flows northward over the sand-dominated sediments near the Danish coast (Longva and Thorsnes, 1997). The SJC is the most erosive of the branches and has the highest concentrations of suspended sediment (Eisma and Kalf, 1987), but is a low-volume water body and hence delivers less sediment to the Skagerrak than the NJC (Longva and Thorsnes, 1997). Relatively small amounts of sediment originate from the major rivers, mainly during spring floods (Kuijpers et al., 1993; Pederstad et al., 1993).

The complicated deglaciation history of the outer Oslo Fjord and the northeastern Skagerrak has been revised several times during the past three decades (e.g., Berglund, 1979; Mörner, 1979; Sørensen, 1979, 1992; Andersen et al., 1995; Lundqvist and Wohlfarth, 2001; Olsen et al., 2001). Based on the results from these studies, Gyllencreutz et al. (2005) concluded that the coring site for MD99-2286 was deglaciated between ca 14.5 and 13.6 cal. kyr. The maximum sea level in the northeastern Skagerrak was immediately after deglaciation about 160–180 m above present sea level (Hafsten, 1983). Due to the rapid isostatic rebound, the sea level was lowered by about 100 m between ca 13.0 and 10.0 cal. kyr, followed by a slower relative sea level fall (Sørensen, 1979; Hafsten, 1983; Lambeck et al., 1998).

Directly after the deglaciation, the Skagerrak was a fjord- or bay-like basin, bordered to the south by large land areas west of present-day Denmark (Stabell and Thiede, 1986; Thiede, 1987). The Skagerrak was subject to a major fresh water input from the final drainage of the Baltic Ice Lake at ca 11.6 cal. kyr (Björck, 1995; Andrén et al., 2002; Björck et al., 2002). Fresh water from the Baltic basin subsequently entered the Skagerrak via outlets across south-central Sweden. This outflow ended ca 10.3 cal. kyr, when the Vänern basin was isolated due to isostatic uplift, and a drainage pathway opened in the southern part of the Baltic (Björck, 1995; Lambeck, 1999).

The opening of the English Channel at ca 8.3 cal. kyr (Jelgersma, 1979; Lambeck, 1995), was considered by Nordberg (1991) to be a necessary condition for the formation of the (southern) Jutland Current and the Norwegian Coastal Current. Biostratigraphic records from the Skagen 3/4 core, drilled onshore northernmost Jutland, Denmark, indicate that this change in the circulation system occurred at 8.5–8.6 cal. kyr (Conradsen and Heier-Nielsen, 1995; Knudsen et al., 1996; Jiang et al., 1997). Major components of the modern circulation system were established in conjunction with a hydrographic shift at ca 6.2 cal. kyr, as interpreted from grain size and biostratigraphic data in cores from Kattegat and Skagen (Conradsen, 1995; Conradsen and Heier-Nielsen, 1995; Jiang et al., 1997). This shift was synchronous with the final drowning of the Jutland Bank (Fig. 1) (Leth, 1996), and is marked by an increased flow of the Jutland Current and thus enhanced saline inflow to the Skagerrak–Kattegat from the North Sea (Conradsen, 1995; Conradsen and Heier-Nielsen, 1995; Jiang et al., 1997). Nordberg (1991) and Nordberg and Bergsten (1988) proposed that this hydrographic shift occurred at 4000 14C years BP (4.6–4.3 cal. kyr), based on 14C dating and biostratigraphic correlation. However, the dating of this event is uncertain judging from the data presented by Nordberg (1991) and Nordberg and Bergsten (1988).

3. Methods

3.1. Grain size

The methods used for grain size analysis of core MD99-2286 were described by Gyllencreutz (2005). Samples consisting of 2.5–3.0 g of freeze-dried sediment were taken every 5 cm from the top of the core to 1500 cm, and between 3100 and 3200 cm. A 10-cm sampling interval was used between 1500 and 3100 cm. The coarse fraction was measured by wet-sieving at 63 μm mesh size. The fine fraction between 63 and 1 μm was analyzed using a Sedigraph 5100. The grain size data were visualized (Fig. 2) by weight percent plotted versus age, of the parameters clay (<2 μm), fine silt (2–10 μm), sortable silt (10–63 μm), and coarse fraction (>63 μm), median grain size and sortable silt median size (McCave et al., 1995). In addition, the entire measured particle size distribution (PSD) (Fig. 2) is here visualized in the form of a three-dimensional PSD surface plot (Beierle et al., 2002). The grain size mode was visually estimated from the PSD surface plot (Gyllencreutz, 2005), by connecting the highest points of the main modal ridge (dotted white line in Fig. 2).

3.2. Magnetic properties

The sampling for magnetic analyses has been made using u-channels (Tauxe et al., 1983; Weeks et al., 1993). A small diameter Bartington coil has been used for the analysis of the low field susceptibility (κ). Anhysteretic remanent (ARM) and isothermal remanent (IRM) magnetizations were measured using high-resolution DC-SQUIDs cryogenic magnetometer placed in the mu-metal-shielded room of LSCE. Measurements were made every 2 cm with a

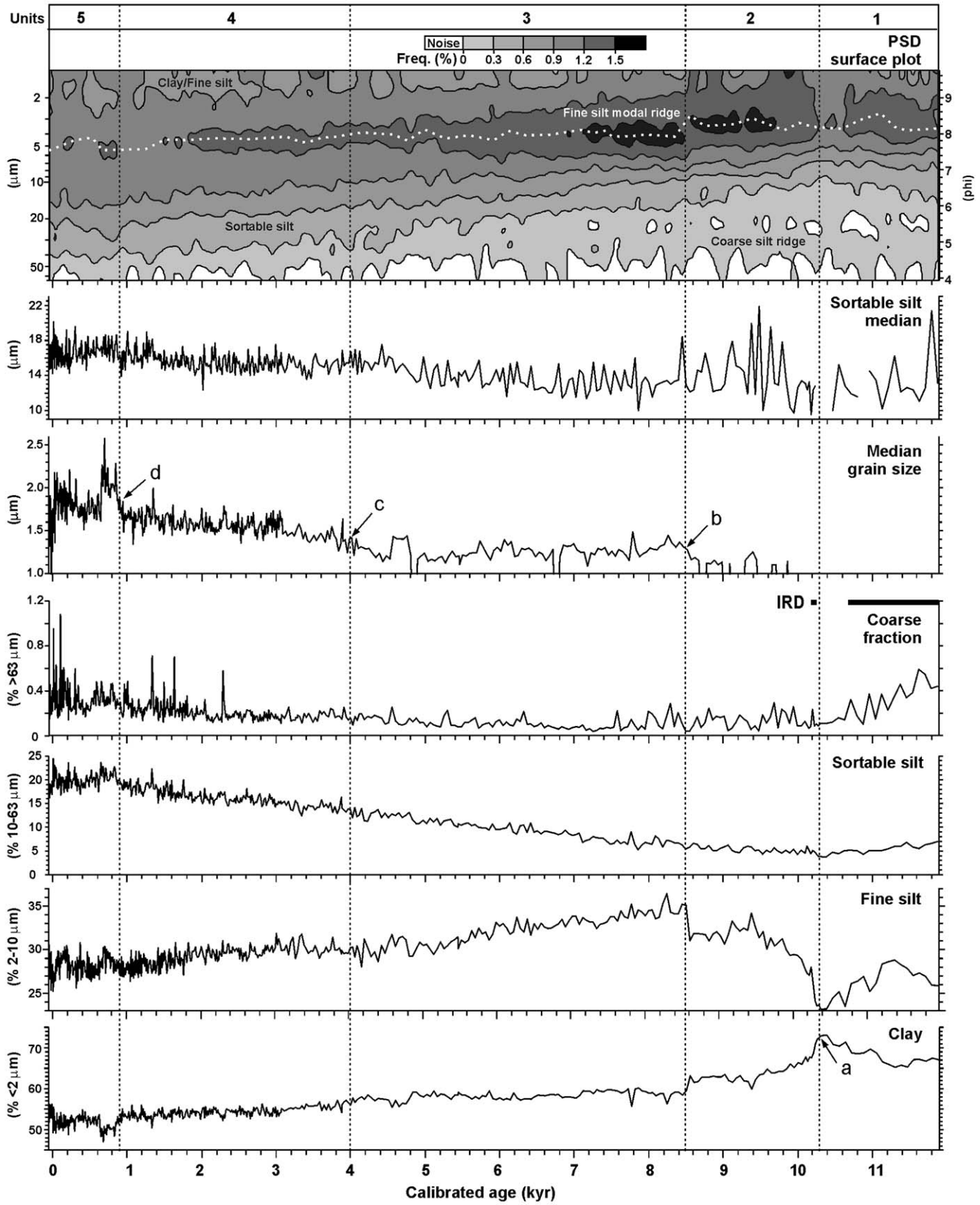

Fig. 2. Low-pass filtered PSD surface plot and individual plots of grain size parameters in core MD99-2286. The location of defined lithological unit boundaries are marked with dotted vertical lines, and the definition points are marked a, b, c, and d with arrows. The white dotted line in the PSD surface plot marks the visually estimated grain size mode from Gyllencreutz (2005). The occurrence of IRD based on visual inspection are marked with black bars in the coarse fraction plot.

resolution of about 4–5 cm. ARM was imparted along the axis of the u-channel by applying a 100 mT alternating field and a 50 μT bias field. During acquisition, the u-channels were translated through the coils at a speed of about 1 cm/s, following Brachfeld et al. (2004). After acquisition, the ARM was stepwise demagnetized using nine successive steps at 10, 15, 20, 25, 30, 40, 50, 60 and 80 mT. Saturated IRM (SIRM) was then acquired in six steps (0.05, 0.1, 0.2, 0.3, 0.5 and 1 T) using a 1.6-m-long pulsed solenoid. Backfield to 0.1 and 0.3 T were applied after saturation in order to calculate the S ratios ($S_{-0.3\,T} = \mathrm{abs}(IRM_{-0.3\,T}/IRM_{1\,T})$ and $S_{-0.1\,T} = \mathrm{abs}(IRM_{-0.1\,T}/IRM_{1\,T})$). SIRM was stepwise demagnetized using the same steps as for ARM. During the demagnetization of ARM and IRM, the u-channel was moving at a speed of about 4 cm/s through the demagnetization coils. All the data were acquired using software developed at LSCE.

Small amounts of sediments (a few mg) were also taken at 20 cm spacing all along the core for the analysis of the hysteresis parameters using an alternating gradient force magnetometer (AGFM 2900). The saturated magnetization (M_s), the saturated remanent magnetization (M_{rs}), the coercive force (H_c), the remanent coercive force (H_{cr}) and the paramagnetic susceptibility (χ_{hf}) were determined. Thermomagnetic analyses were performed on magnetic extracts using a horizontal Curie balance in an argon atmosphere to minimize oxidation.

3.3. Dating

The age/depth model for core MD99-2286 is based on 27 AMS 14C dates, performed on samples of either mollusc shells of known species or mixed benthic foraminifera by the Institute of Particle Physics, ETH, Switzerland. A discussion of the age model construction is given in Gyllencreutz et al. (2005). The radiocarbon dates were calibrated using the CALIB (rev 4.4) software (Stuiver and Reimer, 1993). The calibration data set MARINE98 (Stuiver et al., 1998) was used with a standard reservoir correction of 400 years to facilitate comparison with other records, although it is recognized that the reservoir age may have been greater during the deglaciation (Bard et al., 1990; Bondevik et al., 1999; Björck et al., 2003). The results of the calibrated AMS 14C dates are presented using the probability method (Telford et al., 2004) and are shown in Table 1 and Fig. 3. The bottom of core MD99-2286 at 3198 cm depth was dated to 11.95 cal. kyr (1σ range 12.3–11.7 cal. kyr), and the sedimentation rate increases from 0.06 cm/year in the bottom to 0.9 cm/year in the upper part of the core.

4. Results

4.1. Grain size

About 40–60% of the material in core MD99-2286 is finer than 1 μm, and thus outside the set limit for the sedigraph. The coarse fraction content (>63 μm) is below 1%, throughout the core, but is relatively high in the bottom of the core and decreases rapidly between 11.9 and 10.3 cal. kyr. Microscopic inspection of the coarse fraction shows that the largest grains consist of up to millimetre-sized grains of quartz, feldspar and crystalline rock fragments in samples from 11.9 to 10.7 cal. kyr, and in one single sample at 10.2 cal. kyr. With the exception of the sample at 10.2 cal. kyr, all coarse fraction samples younger than 10.7 cal. kyr generally consist of ca 0.2-mm-sized grains of detrital carbonate and quartz.

The sortable silt median from the bottom of the core until ca 8.5 cal. kyr should be interpreted with caution, as it is based on very little material, which can be seen in the 3D PSD surface plot (Fig. 2) as high amounts of noise (white areas) in the 20–63 μm interval. The major components clay and fine silt show a strong negative correlation in the 11.9–8.2 cal. kyr interval, which probably results from data closure because all parameters are expressed in percent of a total.

Based on grain size, the core has been divided in 5 lithological units, with boundaries at 10.3, 8.5, 4.0, and 0.9 cal. kyr (Gyllencreutz, 2005). The general characteristics and interpretations of these units from Gyllencreutz (2005) are summarized in Table 2.

Unit 1 (11.9–10.3 cal. kyr) is characterized by high and increasing clay content, and by low coarse fraction content with a decreasing component of ice-rafted debris IRD. The grain size median is below 1 μm, and the mode is around 3 μm. Unit 2 (10.3–8.5 cal. kyr) is characterized by rapidly decreasing clay content and a slightly increasing sortable silt content. The coarse fraction content is low, and no IRD occurs in sediments younger than ca 10.2 cal. kyr. Unit 3 (8.5–4.0 cal. kyr) is characterized by a shift towards coarser grain size at 8.5 cal. kyr, relatively stable clay content, gradually increasing sortable silt content, and decreasing modal strength. Unit 4 (4.0–0.9 cal. kyr) is characterized by gradually increasing coarse fraction content, slowly decreasing clay content and decreasing modal strength. The sortable silt content is relatively stable, except for an increase at 1.4 cal. kyr. Unit 5 (0.9 cal. kyr—recent) is characterized by a weak mode, relatively high coarse fraction content, high but decreasing sortable silt content, and low but variable clay content.

4.2. Magnetic properties

All magnetic parameters exhibit similar large wavelength variations (Fig. 4). From the bottom of the core to about 10.5 cal. kyr, the bulk magnetic parameters κ, ARM and IRM first show a slight decrease. They all increase again after 8.5 cal. kyr, reaching a first maximum at about 5.5 cal. kyr. After a new decrease with weak values between 4 and 1.5 cal. kyr, they increase again. This most recent increase in ARM and IRM is of much larger relative amplitude for than for κ. ARM and IRM increase by a factor of 10 and 4, respectively, between 1.4 and about

Table 1
AMS 14C dating of core MD99-2286

Laboratory reference	Depth (cm)	δ^{13}C vs PDB		^{14}C age (Libby h.l.)		Age range (cal y BP) probability method			Dated material[a]	Weight	Type[b]
		(‰)	$\pm1\sigma$	(14C y BP)	$\pm1\sigma$	Max (1σ)	Median	Min (1σ)		(mg)	
(ETH-24953)	115.5	−3.8	1.2	785	50	480	424	378	*Scaphander* sp.	27.78	g,wh
(ETH-25546)	185.5	2.0	1.2	800	55	494	436	393	*Yoldiella lucida* (Lovén, 1846)	8.85	b,wh
ETH-24001	268	1.7	1.2	535	50	252	166	113	*Ennucula tenuis* (Montagu, 1803)	26.1	b,wh
ETH-24397	319.5	1.8	1.2	730	45	417	372	320	*Thyasira equalis* (Verrill and Bush, 1898)	49.67	b,br
(ETH-26937)	319.5	0.5	1.2	1095	55	701	652	613	Foraminifera (mixed fauna)	11.86	f
ETH-25547	370.5	0.7	1.2	900	60	548	513	467	*Nucula tumidula* (Malm, 1861)	9.55	b,br
(ETH-26388)	410.5	0.1	1.2	1270	50	877	814	761	Foraminifera (mixed fauna)	13.07	f
ETH-26938	481.5	2.7	1.2	1225	55	824	768	699	Foraminifera (mixed fauna)	16.77	f
(ETH-26939)	561	−0.1	1.2	1510	50	1115	1057	992	Foraminifera (mixed fauna)	18.57	f
ETH-26940	640.5	0.8	1.2	1530	50	1146	1080	1024	Foraminifera (mixed fauna)	16.23	f
(ETH-25955)	700.5	2.3	1.2	1915	55	1518	1458	1398	Foraminifera (mixed fauna)	16.42	f
ETH-25956	801	−0.2	1.2	1915	55	1518	1458	1398	Foraminifera (mixed fauna)	18.04	f
(ETH-26389)	901	0.5	1.2	2155	50	1808	1744	1690	Foraminifera (mixed fauna)	19.29	f
ETH-26390	1001	−0.5	1.2	2175	50	1819	1766	1705	Foraminifera (mixed fauna)	15.51	f
ETH-26941	1070.5	3.0	1.2	2440	55	2138	2076	1997	Foraminifera (mixed fauna)	11.62	f
ETH-26418	1200.5	1.4	1.2	2765	60	2572	2493	2360	Foraminifera (mixed fauna)	12.56	f
ETH-27241	1360.5	0.0	1.2	2975	55	2789	2752	2704	Foraminifera (mixed fauna)	14.87	f
(ETH-26419)	1460.5	1.3	1.2	3390	60	3334	3256	3192	Foraminifera (mixed fauna)	14.05	f
(ETH-27242)	1660.5	−1.7	1.2	3895	60	3952	3861	3775	Foraminifera (mixed fauna)	18.1	f
ETH-26137	1826	1.0	1.2	4120	60	4252	4173	4081	*Polinices montagui* (Forbes, 1838)	16.73	g,wh
ETH-24003	2377	1.3	1.2	6255	65	6773	6698	6628	*Portlandia intermedia* (M. Sars, 1859)	42.6	b,br
ETH-25548	2676.5	3.4	1.2	7955	70	8478	8410	8335	*Pseudamusium septemradiatum* (Müller, 1776)	62.37	b,br
(ETH-25549)	2681.5	2.9	1.2	7710	60	8262	8163	8099	*Pseudamusium septemradiatum* (Müller, 1776)	100.02	b,br
ETH-25550	3100.5	−0.6	1.2	9620	70	10585	10332	10145	*Pseudamusium septemradiatum* (Müller, 1776)	44.68	b,br
ETH-24004	3119	1.1	1.2	9955	85	11080	10734	10373	*Bathyarca glacialis* (Gray, 1824)	25.5	b,br
ETH-25551	3129.5	−2.0	1.2	9910	70	11003	10696	10354	*Cryptonatica affinis* (Gmelin, 1791)	25.77	g,br
ETH-24005	3198	1.4	1.2	10715	80	12306	11954	11678	*Portlandia intermedia* (M. Sars, 1859)	134.5	b,br

Laboratory reference codes in parentheses mark samples omitted from the age model due to presumed reworking of fossils.

[a]Mollusc names following CLEMAM (Le Renard, 2005).

[b]Type abbreviations: g = gastropod, b = bivalve, f = benthic foraminifera, wh = whole, br = broken.

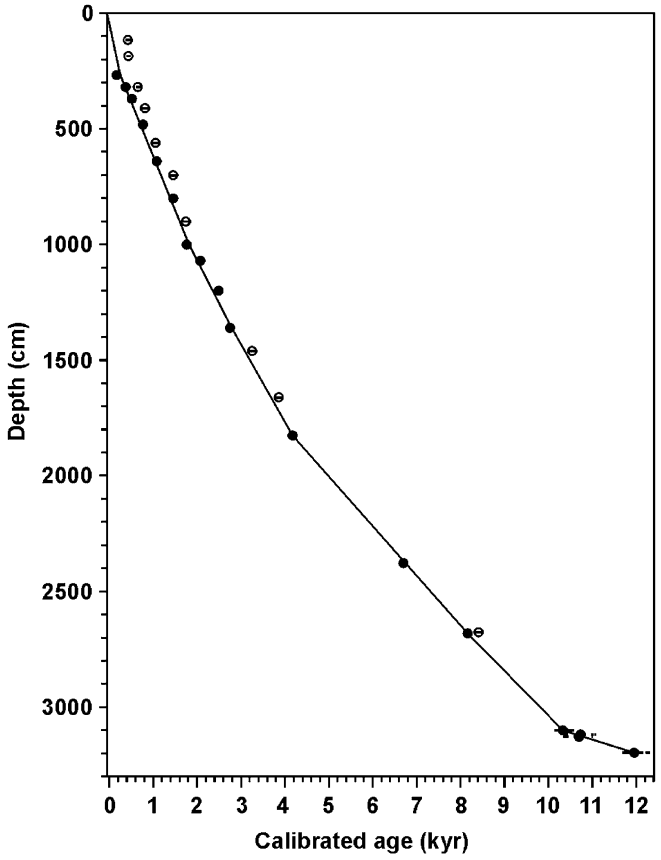

Fig. 3. Age/depth model for core MD99-2286 based on 27 AMS 14C dates. The age model is shown with a line connecting black dots. Open circles mark age estimates excluded from the age model because of presumed sediment reworking. Error bars marked by horizontal lines through the dates denote 1σ calibrated age ranges (see also Table 2). Several error bars are smaller than the dots.

0.9 cal. kyr while κ increases only by a factor of 1.3. The bulk magnetic parameters remain constant as a first approximation during the last 900 years.

The two S ratios show similar trends, between 0.64 and 0.82 for S ratio$_{-0.1\,T}$ and between 0.84 and 0.96 for S ratio$_{-0.3\,T}$. They both show a continuous decrease from the bottom of the core to about 7 cal. kyr indicating an increase in the coercivity. They then increase toward a maximum around 5.5 cal. kyr, decrease again toward a broad minimum between about 4 and 1.5 cal. kyr. The two S ratios increase rapidly again between 1.5 and 0.9 cal. kyr and then remain approximately constant at high values illustrating the dominance of low coercivity magnetic minerals.

The generally high values of the S ratio (>0.84) indicate that magnetite is probably the most abundant magnetic mineral in core MD99-2286. However, some significant contribution of "harder" magnetic minerals is observed in the intervals of the lowest S ratios. This hard component may be carried by hematite as suggested by Lepland and Stevens, or by greigite. The origin of hematite in this area is not clear but it may be present in rocks from Scandinavia. Lepland and Stevens (1996) noticed that this component is more abundant in samples showing a "Norwegian" magnetic signature. Greigite is present in lake sediments from Scandinavia (Snowball, 1991) and may also be present, in low concentration, in core MD99-2286. Both natural hematite and greigite are characterized by higher values of magnetic parameters such as SIRM/κ, M_r/M_s and H_{cr} than observed here (Snowball, 1991). It is therefore difficult to distinguish minor quantities of these minerals and to clearly identify them in a magnetite rich sediment.

In order to identify the magnetically hard minerals, we used temperature spectra as magnetite looses its magnetization around 580 °C, hematite around 690 °C and greigite is unstable around 320–350 °C. We performed thermomagnetic analyses on magnetic extract. A representative curve from the 1053–1321 cm depth interval, corresponding to 1.96–2.68 cal. kyr where the S ratio is the lowest is shown in Fig. 5. The decrease of the magnetization upon heating is regular until about 545 °C, where it speeds up until 600 °C is reached. A very small component is present between 600 and 620 °C. Except for the latter, the curve is typical of magnetite. The cooling curve is perfectly reversible from 620 to 540 °C, and then smoothly comes back to room temperature above the heating curve. No transition typical for greigite is observed at 320 °C, but the lack of reversibility may indicate some mineralogical transformations and/or changes in the magnetic grain size upon heating. The thermal treatment did not give a clear identification of the magnetically hard minerals. However, the analysis shows that if greigite and/or hematite is present during intervals of low S ratios, it is only in small concentration.

The proxy most commonly used to estimate size of magnetites is the ARM/κ ratio and also ARM/IRM ratio. The latter concerns only remanent magnetizations and is thus independent from paramagnetic and diamagnetic components. IRM/κ ratio is also used as it varies in the same way as the others in case of changes in grain size of magnetites. All these ratios show the same pattern in core MD99-2286: rather constant values or slight decrease (i.e. increase in magnetic grain size) from the bottom of the core to about 8.5 cal. kyr. This is followed by a slight increase with a broad maximum around 5.5 cal. kyr, a decrease (coarser magnetic grains) between 4.5 and 4 cal. kyr, a new increase between 1.5 and 0.9 cal. kyr and then constantly high values illustrating the finest magnetic grain sizes in the core. This pattern is confirmed by the hysteresis parameters combined as suggested by Day et al. (1977), i.e. as the magnetization ratio M_{rs}/M_s and the coercivity ratio H_{cr}/H_c (Fig. 6).

In summary, we can distinguish different time intervals, each characterized by different magnetic properties. We observe

(a) from about 12 to 8.6 cal. kyr, weak bulk parameters associated to coarse magnetic grains and increase in magnetic coercivity;
(b) from about 8.5 to 6.4 cal. kyr, a progressive increase in the bulk magnetic parameters and in the grain size proxies, low S ratios values (high coercivities);

Table 2
Summary of the results and interpretations of the MD99-2286 grain size record from Gyllencreutz (2005)

Unit (cal. age in kyr)	Grain size observations (trends described in direction towards younger sediments)	Paleoceanographic interpretation
Unit 1 (11.9–10.3)	Mode: variable around 3 μm Median: below 1 μm Sort. silt median: highly variable, less reliable Coarse fraction: decreasing content of IRD Sort. silt: low, slightly decreasing Clay: high and rapidly increasing	Ice berg calving in the Oslofjord clay-ceased 10.7–10.2 kyr. Deposition of clay-rich sediments from the Baltic basin via outlets on Swedish west coast. South Jutland Current absent
Unit 2 (10.3–8.5)	Mode: around 3 μm, increasing strength Median size: varying around 1 μm Sort. silt median: highly variable, less reliable Coarse fraction: low and variable Sortable silt: low, slightly increasing Clay: high but rapidly decreasing	Decreasing clay content due to closing of the Otteid-Stenselva outlet at 10.3 kyr. Postglacial normal marine sedimentation begins. South Jutland Current absent
Unit 3 (8.5–4.0)	Mode: shifted to ca 4 μm, decreasing strength Median size: low and relatively stable Sort. silt median: gradually increasing Coarse fraction: low and stable Sortable silt: slowly increasing Clay: relatively stable	Modern circulation pattern begins at 8.5 kyr, due to opening of English Channel and Danish straits, increased Atlantic inflow and transgression of s. North Sea. Stronger bottom current
Unit 4 (4.0–0.9)	Mode: coarsening to 5 μm, decreasing strength Median size: higher than unit 3 Sort. silt median: stable, increase at 1.4 kyr Coarse fraction: gradually increasing Sortable silt: slowly increasing Clay: slowly decreasing	Strengthening of the Jutland Current and development towards the modern type of sedimentation pattern. Sediments mostly from the Atlantic Current and the southern North Sea
Unit 5 (0.9–recent)	Mode: very weak around 5 μm Median size: highest in the record Sort. silt median: high and variable Coarse fraction: high and variable Sortable silt: high, slowly decreasing Clay: low but variable	Circulation system modified by regional climate, especially general wind directions and storm frequency. Strong and variable South Jutland Current

(c) from about 6.4 cal. kyr to about 4.7 cal. kyr, a broad maximum in the bulk magnetic parameters with low coercivities and in the magnetic grain size proxies;
(d) from 4 to 1.5 cal. kyr, a minimum in κ, ARM, IRM, and in the grain size proxies, and relatively weak S ratios (indicating contribution of slightly higher coercivities);
(e) last 900 years, a stable period with the largest amount of the finest low coercivity magnetic grains encountered in the core.

5. Discussion

5.1. Grain size

The MD99-2286 grain size record has been discussed in detail by Gyllencreutz (2005), and the main results are listed in Table 2.

In a PSD surface plot, a persistent mode will resemble a series of peaks appearing as a ridge. The width of the modal ridge can be used as a crude measure of the sorting, where a narrow mode is indicative of well sorted material (Kranck and Milligan, 1991). The relative changes in width of the modal ridge in the 3D PSD surface plot, shows that the sorting has decreased continuously since ca 8.5 cal. kyr.

The 11.9–10.3 cal. kyr interval (unit 1) is characterized by a relatively significant amount of coarse fraction interpreted as IRD derived from the Oslo Fjord. The decreasing trend illustrates a decrease in the iceberg calving which ceases at about 10.2 cal. kyr. The increasing clay content during the same period was probably the result of outflow of sediment-loaded meltwater from the Baltic basin across south-central Sweden through outlets that opened a few hundred years after the final drainage of the Baltic Ice Lake ca 11.6 cal. kyr. Similar units with high clay contents in the Horticultural Garden core in Gothenburg and in the Solberga-2 core were subsequently formed when the meltwater drainage route migrated southward due to the isostatic uplift gradient (Gyllencreutz, 2005). The age range of the Otteid-Stenselva closure correlates with the end of the clay increase in core MD99-2286 at 10.3 cal. kyr, suggesting that the Otteid-Stenselva was the most important of the Baltic drainage routes for the sedimentation at the MD99-2286 site. The low sortable silt content indicates

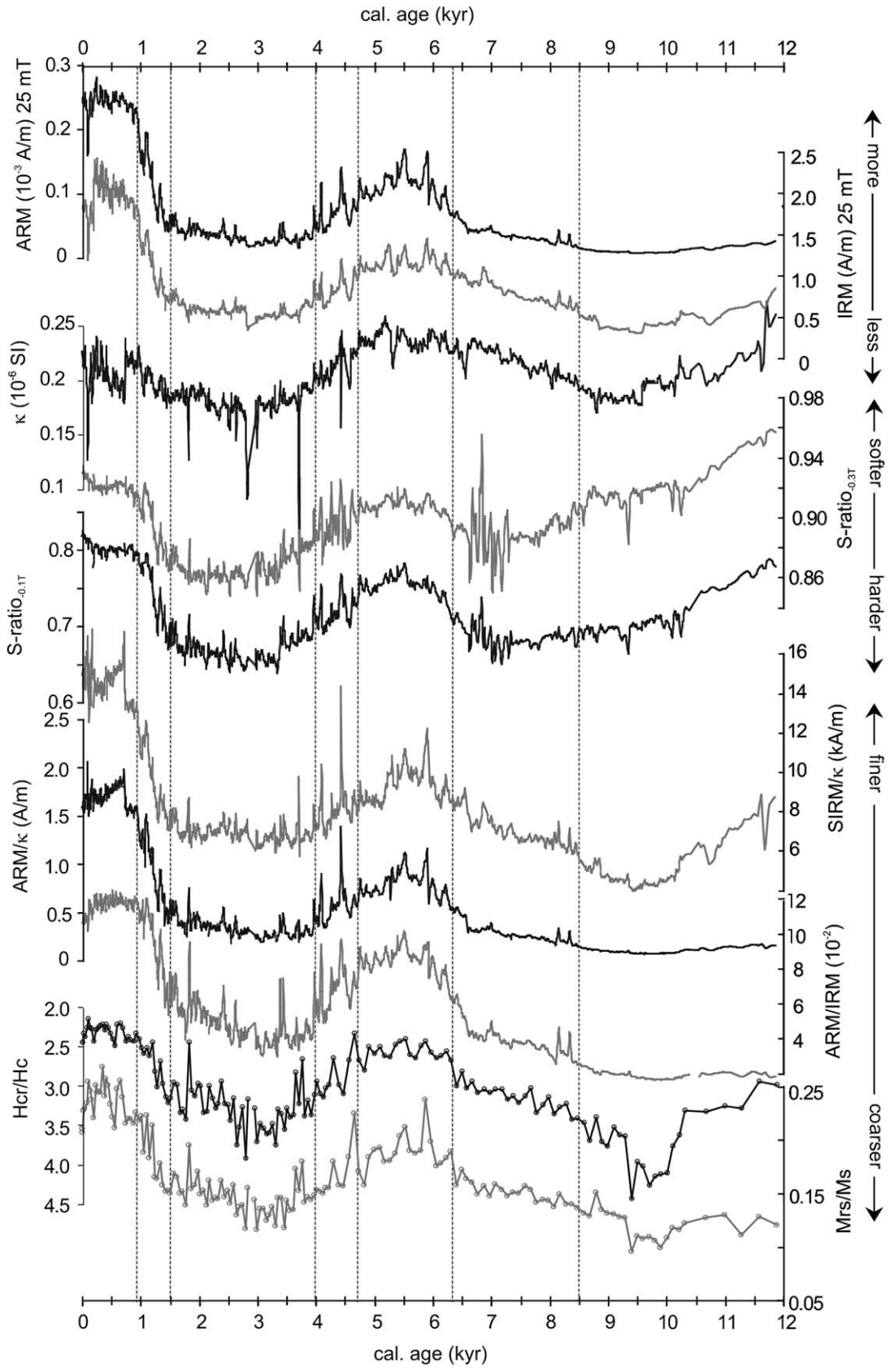

Fig. 4. Mineral magnetic properties of core MD99-2286 plotted versus age. Boundaries between defined time intervals with characteristic magnetic properties are indicated with vertical lines.

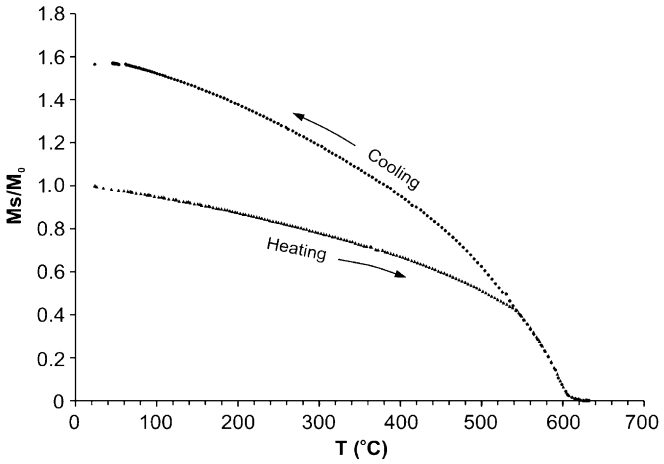

Fig. 5. Thermomagnetic curves obtained from magnetic extracts, showing the normalized evolution of the saturated magnetization versus temperature. The curves are representative for the depth interval 1053–1321 cm (1960–2680 kyr) in core MD99-2286.

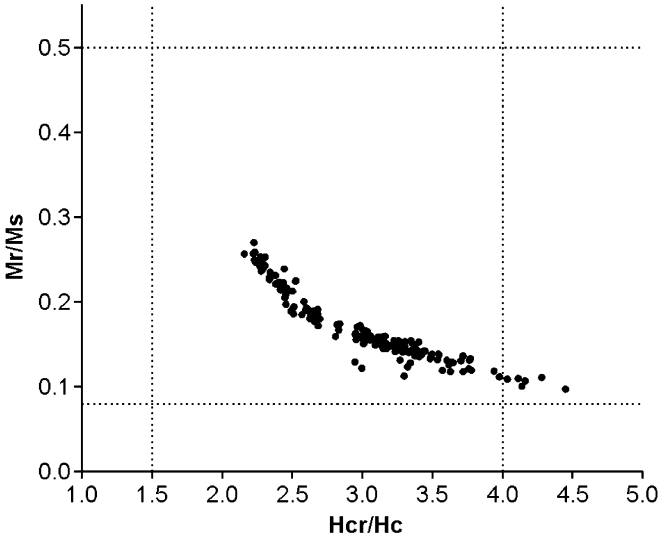

Fig. 6. Hysteresis parameters for core MD99-2286 plotted in a Day diagram (Day et al., 1977).

that the current speed in the Skagerrak was low during this time interval.

The low current velocities persisted to the end of the 10.3–8.5 cal. kyr interval (Unit 2). During that period, the Skagerrak gradually became influenced by a full-interglacial marine sedimentation governed by Atlantic inflow via the NJC. This is illustrated by the decrease in the clay content, resulting from an associated decreasing influence of distal glacial-marine sediments. At the end of this period, the distinct change in the grain size properties (increase in median grain size and in fine silt, decrease in the clay content and variance of the sortable silt median) indicates that the sedimentary environment in the Skagerrak was altered by a hydrographic shift at 8.5 cal. kyr. This can be correlated with previous observations of changes in grain size, foraminifera, or diatoms in cores from the Norwegian Channel and the Skagerrak–Kattegat region, which were suggested to mark the establishment of the modern hydrographic circulation system in the Skagerrak at that time (Nordberg, 1991; Conradsen and Heier-Nielsen, 1995; Knudsen et al., 1996; Jiang et al., 1997). The development towards the modern type of circulation includes (1) a general strengthening of the current system by increased Atlantic inflow, (2) the opening of the Danish straits permitting outflow of relatively fresh water from the Baltic Sea to the Kattegat, (3) the opening of the English Channel enabling Atlantic water inflow from the south, and (4) transgression of former land areas in the southern North Sea, which permitted formation of the SJC (Gyllencreutz, 2005).

During the following period (8.5–4.0 cal. kyr; Unit 3), the gradual increase in the sortable silt median and in the modal ridge of the PSD surface plot indicates a gradually stronger current. This evolution is enhanced between 4 and 0.9 cal. kyr (Unit 4) and corresponds to an overall coarsening of the sediment with a decrease in fine silt and a small increase in coarse fraction.

The modern surface current pattern in the Skagerrak–Kattegat was established in conjunction with a hydrographic shift to higher energy conditions during the mid-Holocene (Nordberg and Bergsten, 1988; Nordberg, 1991; Conradsen and Heier-Nielsen, 1995; Conradsen, 1995; Jiang et al., 1997). The timing of this shift is not clear, and has been suggested to ca 4.6–4.3 cal. kyr based on results from cores in the south eastern Skagerrak and the Kattegat (Nordberg and Bergsten, 1988; Nordberg, 1991), and to ca 6.2–5.9 cal. kyr based on results from the Skagen 3/4 core (Conradsen and Heier-Nielsen, 1995; Jiang et al., 1997) and from piston cores from the Kattegat (Conradsen, 1995). Gyllencreutz (2005) suggested that the hydrographic shifts recorded in the interval 6.2–3.8 cal. kyr in core MD99-2286 and in other sites in the Skagerrak–Kattegat belong to a continuous hydrographic development. The sedimentary changes during this relatively long interval are differently manifested in different parts of the Skagerrak–Kattegat region, depending on its complex circulation system and differences in sedimentary environment between the investigated sites.

The sortable silt median and the coarse fraction are relatively stable throughout the record after an increase in both parameters at 1.3 cal. kyr. This indicates that the modern strength and variability of the bottom current has prevailed since about 1.3 cal. kyr.

During the most recent period of time (0.9 cal. kyr to present; Unit 5), a distinct feature is observed between 0.9 and 0.6 cal. kyr with remarkably high values in median grain size, and high coarse fraction, sortable silt and fine silt, and a low clay content (Fig. 2). Despite the increased sortable silt content, the sortable silt median remains largely unaffected (Fig. 2), implying that the change is not related to bottom current velocity at the deposition site. The event around 0.9 cal. kyr has been observed in three other cores from the southern flank of the Skagerrak, and

was interpreted as the result of increased winter storminess during a short-term cold spell, in an otherwise warm climate phase with little storm activity (Hass, 1996).

The sortable silt content in core MD99-2286 starts a decreasing trend for the first time at ca 0.8 cal. kyr, lasting to the present, indicating a small shift in sedimentation. The coarse fraction shows a trend towards higher and more variable values and the sortable silt median shows high and variable values during the same interval, indicating relatively strong bottom currents in the north-eastern Skagerrak. The high variability during the last 800 years in the MD99-2286 grain size record indicates a current system significantly affected by regional climatic variability.

5.2. Magnetic properties

When only magnetite is present, coarse grains should be associated with higher S ratios than the fine grains. The opposite relationship is observed here and was also noticed by Lepland and Stevens (1996) on surface sediments. Although other magnetic minerals than magnetite could not be identified by thermomagnetic curves, we suggest that during the time intervals characterized by coarser grains of magnetite, magnetically harder minerals are also present and contribute to the magnetic signal.

On the basis of the long-term changes in magnetic parameters showed in Fig. 4, we can identify two main magnetic assemblages. The first one is characterized by low bulk κ, SIRM and ARM values, and low SIRM/κ and S ratio values and is thus constituted of coarse grained magnetite mixed with variable amounts of high coercivity mineral. The second assemblage gives high values of κ, SIRM/κ and ARM, high values of the magnetic grain size proxies ARM/κ, SIRM/κ, ARM/SIRM, H_{cr}/H_c and M_{rs}/M_s and low S ratio values. This illustrates high amounts of fine grained magnetite.

These assemblages are similar to those observed in modern sediments by Lepland and Stevens (1996) from the northern Skagerrak. Based on the geographical distribution of the surface samples, the authors have attributed the first assemblage to a "Norwegian" type detrital supply and the second one to a "Danish" supply. At present, the Norwegian population is distributed along the Norwegian coast and in the northeastern Skagerrak, while the Danish population occupies the central part of the Skagerrak. Core MD99-2286 was recovered from a location at the border between the two populations (Fig. 7). In this core, the two assemblages are successively present in time. They are sometimes mixed and show transitional changes as shown in Fig. 8 where SIRM/κ ratio is shown versus S ratio, with the evolution in time illustrated by arrows. At the bottom of the core around 11.9 cal. kyr, fine grained magnetite with a markedly low content of magnetically hard minerals are present (cluster A), and move rapidly towards a mixture of coarse MD magnetite grains and small amounts of magnetically hard minerals (cluster B). Between 8.5 and 6.4 cal. kyr, slightly finer magnetite grains with an increasing amount of magnetically hard minerals are delivered to the site. Between 6.4 and 4.7 cal. kyr, finer magnetite grains with less magnetically hard minerals were deposited. Coarser magnetite with the highest content of magnetically hard minerals (S ratio$_{-0.3\,T}$ varies between 0.84 and 0.9) is observed between 1.5 and 4.2 cal. kyr, reaching a maximum between 3 and 2 cal. kyr. This population is typical for the "Norwegian type" defined by Lepland and Stevens. The present day period is characterized by clear Danish type sediments. This indicates that the sediment transport is dominated for the last ca 900 years by North Atlantic water and the Jutland Current.

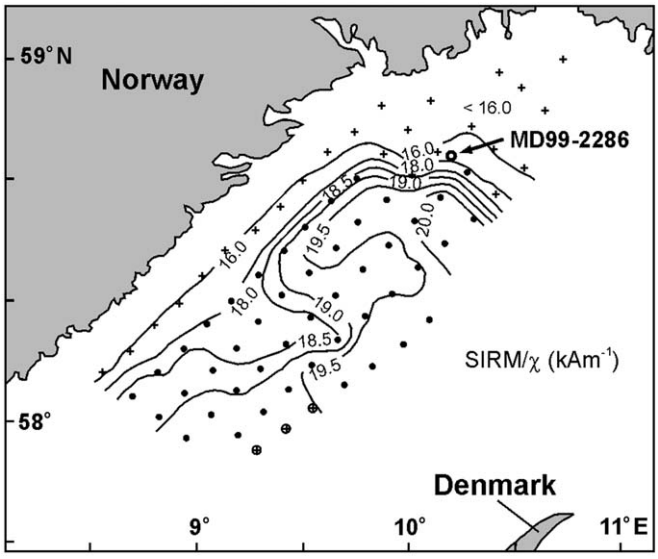

Fig. 7. The geographical distribution of the ratio of SIRM to χ from Lepland and Stevens (1996). Core MD99-2286 (circle and arrow) was recovered from a location at the border between the Danish (points) and Norwegian (crosses) mineral magnetic populations defined by Lepland and Stevens (1996). The three circled crosses within the Danish population mark samples with a remarkably high content of MD-grains (Lepland and Stevens, 1996). Modified after Lepland and Stevens (1996, Fig. 6 and 7).

5.3. Sediment source variations

In the following discussion, the two principal magnetic provinces in the Skagerrak are referred to as Danish and Norwegian for simplicity reasons (as originally termed in Lepland and Stevens, 1996). These terms are equivalent to the "North Sea/Atlantic Ocean" (Danish) and the "Scandinavian/Baltic" (Norwegian) provinces named by Longva and Thorsnes (1997).

The sediment contribution from Scandinavia and the Baltic Sea has been estimated to about 15% of all deposited sediments in the Skagerrak (Longva and Thorsnes, 1997). Because of the intense current mixing in the eastern Skagerrak cyclonic gyre, it is therefore likely that particles from the Atlantic Ocean and the North Sea ("Danish" sediments) constitute the bulk of the sediments

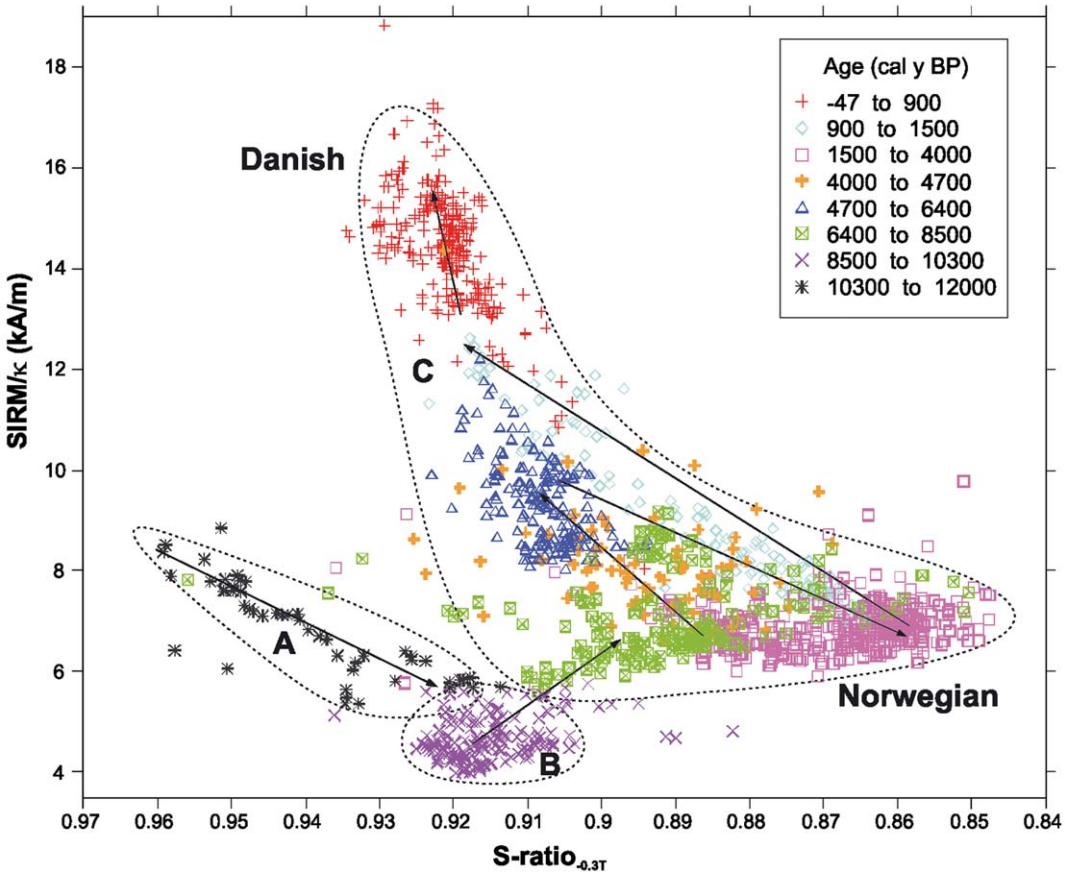

Fig. 8. The relationship between SIRM/κ and *S* ratio in core MD99-2286. The samples are plotted in age classes with different colors and symbols, with boundaries identical to the defined time intervals of characteristic grain size and magnetic properties (see Figs. 2 and 4). The three major clusters discussed in the text are marked A, B, and C, and the general development with time is indicated with arrows. Danish sediments have less magnetically hard minerals (lower *S* ratio) and finer magnetic grain size (higher SIRM/κ) than Norwegian sediments, and the magnetic grain size is the most diagnostic of these parameters (Lepland and Stevens, 1996).

even in the Norwegian province. The reason for the distinct magnetic difference between the two populations, despite the low concentration of Norwegian particles in the bulk sediment, may be that the Danish sediments to a large extent are derived from sedimentary rocks of the North Sea, whereas the Norwegian sediments are predominantly of metamorphic and plutonic origin (Longva and Thorsnes, 1997). In the surface sediment study by Lepland and Stevens (1996), the spatial distribution of the sediments with a Norwegian mineral magnetic signature closely follows the path of the Baltic Current in the north-eastern Skagerrak, and its continuation as the Norwegian Coastal Current after mixing with the Jutland Current. The magnetically Danish surface sediments occupy the central and southern Skagerrak, where the Jutland Current flows. Assuming this relationship between currents and mineral magnetic properties has been valid further back in time, the mineral magnetic signature could indicate the relative influence of the major currents governing the Skagerrak sedimentation, i.e. the inflow of Atlantic water via the Jutland Current (controlling the Danish signature) and the Baltic Current and Norwegian Coastal Current (controlling the Norwegian signature). These are the same principal water masses that determine the sea-surface salinity in the Skagerrak, as various amounts of relatively fresh outflow water from the Baltic dilute the more saline water from the Jutland Current (Rodhe, 1996; Jiang et al., 1998). Variations in the current pattern inferred from the mineral magnetic signal should therefore be consistent with interpreted changes in current pattern based on sea surface salinity variability in the Skagerrak. Changes in the Skagerrak sea-surface salinity have been reconstructed by Jiang et al. (1998) for the entire Holocene except the last ca 1000 years, using diatom transfer functions based on data from the Skagen 3/4 core.

Between 11.3 and 10.3 cal. kyr, the magnetic fraction evolves from pure magnetite of medium size (cluster A) to a little higher coercivities and coarser grains (cluster B in Fig. 8). This may illustrate progressively increasing supply of glacial sediments from south western Sweden and southern Norway. At the same time, between 11.3 and 10.3 cal. kyr, the clay content is high and increasing, and the sortable silt is low and slightly decreasing with younger sediments. This interval was interpreted to reflect outflow

Baltic water from the Swedish west coast (Gyllencreutz, 2005), mainly through the Otteid-Stenselva strait. A large part of the sediments transported by the Baltic outflow to the Skagerrak were likely glacially eroded material re-deposited from the Vänern basin. Therefore, we suggest that the mineral magnetic properties between 11.9 and 11.3 cal. kyr reflects re-deposited glacial sediments from southern Norway and western Sweden, and that the magnetic signature between 11.3 and 10.3 reflects re-deposition of glacial sediments in the Vänern Basin transported by the Baltic outflow.

The relatively constant relationship between SIRM/κ (low) and S ratio (high) between 10.3 and 8.6 cal. kyr (cluster B in Fig. 8) could be explained by a different current pattern compared to the period after 8.6 cal. kyr. Before about 9 cal. kyr, the northward current along the Swedish west coast was likely significantly weaker, because the passageway through the Danish straits was closed (Björck, 1995; Lambeck, 1999), although a drainage route for Baltic water existed with a connection somewhere in the southern Kattegat (Björck, 1995). The Great Belt is the deepest of the three straits connecting the Baltic Sea and the Kattegat–Skagerrak, and accounts for more than 75% of the water exchange between these seas (Bennike et al., 2004). Based on isostatic modeling results, Lambeck (1999) suggested that full marine conditions were established in the Danish straits around 8.7–8.2 cal. kyr (Gyllencreutz, 2005, Table 1). The oldest reported marine shells from the Great Belt were dated to 8.1 cal. kyr, but brackish water conditions prevailed for some centuries before that (Bennike et al., 2004).

The SJC was virtually absent before 8.6 cal. kyr, based on the consistent results from the grain size record of core MD99-2286 (Gyllencreutz, 2005) and the Skagen 3/4 core (Jiang et al., 1997; Knudsen et al., 1996) . In the absence of the Baltic Current and the SJC, the circulation and sedimentation in the Skagerrak was likely dominated by the NJC. This is supported by foraminifera and diatom data from the Skagen 3/4 core, indicating that the sediments were derived from a westerly source between 9.5 and 8.5 cal. kyr (Conradsen and Heier-Nielsen, 1995; Jiang et al., 1997; Gyllencreutz, 2005, Table 1). The stable SIRM/κ and S ratio values between 10.3 and 8.6 is therefore suggested to reflect sediments dominated by sources west of the Skagerrak.

The period between 8.5 and 8.2 appears to represent a transitional phase between the two periods of different SIRM/κ and S ratio relationships. Therefore, we suggest that a source area system different from the present prevailed between 11.9 and 8.6 cal. kyr, followed by a short transitional period, and that the present-day system of Danish and Norwegian sediment source mixing was established at about 8.2 cal. kyr. The change in SIRM/κ and S ratio$_{-0.3\,T}$ properties at 8.6–8.5 cal. kyr appears to be synchronous with the major hydrographic shift indicated by the grain size data, which was interpreted to reflect the establishment of the modern circulation system and opening of the English Channel and the Danish Straits (Gyllencreutz, 2005). The mineral magnetic data, coupled with the grain size analyses thus support a major shift in the Skagerrak–Kattegat hydrography at 8.6–8.5 cal. kyr.

It is clear from Fig. 8 that the magnetic properties of the sediments younger than 8.2 cal. kyr evolves with time and show various mixing between the two end-members defined from surface sediments by Lepland and Stevens (1996). The mineral magnetic parameters indicate a high influence of the Baltic Current and of the currents along the Swedish and Norwegian coasts (Norwegian type) between 8.5 and 6.4 cal. kyr, and between 4.0 and 1.2 cal. kyr. The period between 6.2 and 4.7 cal. kyr was characterized by weaker Baltic outflow and enhanced transport by the Jutland Current (Danish type). This result is consistent with the interpreted acceleration of the Jutland Current at ca 6.2–5.9 cal. kyr, as previously suggested by Jiang et al. (1997), Conradsen and Heier-Nielsen (1995) and Conradsen (1995). The MD99-2286 magnetic record from ca 0.9 cal. kyr until the present is characterized by a strongly Danish mineral magnetic signal, indicating a sediment transport dominated by Atlantic water and the Jutland Current.

The circulation changes indicated by the MD99-2286 magnetic record is in general agreement with the interpreted changes in current pattern based on the diatom-based reconstruction of sea-surface salinity from the Skagen 3/4 core by Jiang et al. (1998). They suggested a high salinity between 11.2 and 10.8 cal. kyr (9800 and 9500 14C y BP, Petersen, 2004), reflecting strong influence of NJC and reduced Baltic outflow, followed by generally low salinity in the period 10.8–6.6 cal. kyr (9500–5900 14C y BP, Petersen, 2004), reflecting strong influence of Baltic water, and stronger influence of currents along the Swedish and Norwegian coast. Jiang et al. (1998) further suggested that the interval between 6.4 and 5.4 cal. kyr (5700 and 4700 14C y BP, Petersen, 2004) was characterized by high salinity, reflecting a drier climate and acceleration of the SJC. The Norwegian magnetic signal between 4.7 and 1.2 cal. kyr is not correlated to any salinity changes in the Skagen 3/4 core, but is in agreement with the interpreted weakening of the SJC between 3.4 and 2.2 cal. kyr (Table 1) (Jiang et al., 1997). The trend towards lower salinity after 1.1 cal. kyr (1200 14C y BP, Petersen, 2004) suggested by Jiang et al. (1998) is in agreement with the decreasing trend in SIRM/κ during the last 0.9 cal. kyr of core MD99-2286, indicating a decreasing Danish/increasing Norwegian magnetic signature.

6. Conclusions

High-resolution grain size and mineral magnetic analyses of the Skagerrak core MD99-2286 show Lateglacial and Holocene changes in circulation, sedimentation and provenance for the Skagerrak sediments. The magnetic signal is dominated by pseudo-single domain to multi-domain magnetite. Two main magnetic assemblages can be

distinguished, similar to the "Norwegian" and "Danish" populations observed by Lepland and Stevens (1996) in the northern Skagerrak surface sediments. The different compositions of these two magnetic assemblages are attributed to differences in sediment source areas and transport pathways. The "Danish" provenance is totally dominated by sediments from the southern North Sea and the Atlantic Ocean, mainly transported by the North and South Jutland Current. Most of the "Norwegian" sediments are also derived from the southern North Sea and the Atlantic Ocean, but with important contributions from the Baltic Sea and reworked coastal sediments in Sweden and Norway, mainly transported by the Baltic Current and currents along the coasts of western Sweden and southern Norway.

Based on the mineral magnetic properties and grain size variability in core MD99-2286 and previous paleoceanographic studies from the Skagerrak–Kattegat, the following conclusions can be drawn about the history of circulation, sedimentation and provenance in north-eastern Skagerrak since Lateglacial times. A schematic compilation of this development is presented in Fig. 9.

- *Between about* 12 *and* 11.3 *cal. kyr*: Sedimentation in the north-eastern Skagerrak was strongly influenced by meltwater discharge carrying re-deposited glacial sediments from southern Norway and western Sweden; a calving ice front was still present in the Oslo Fjord. The sediment transport pattern changed as a result of the

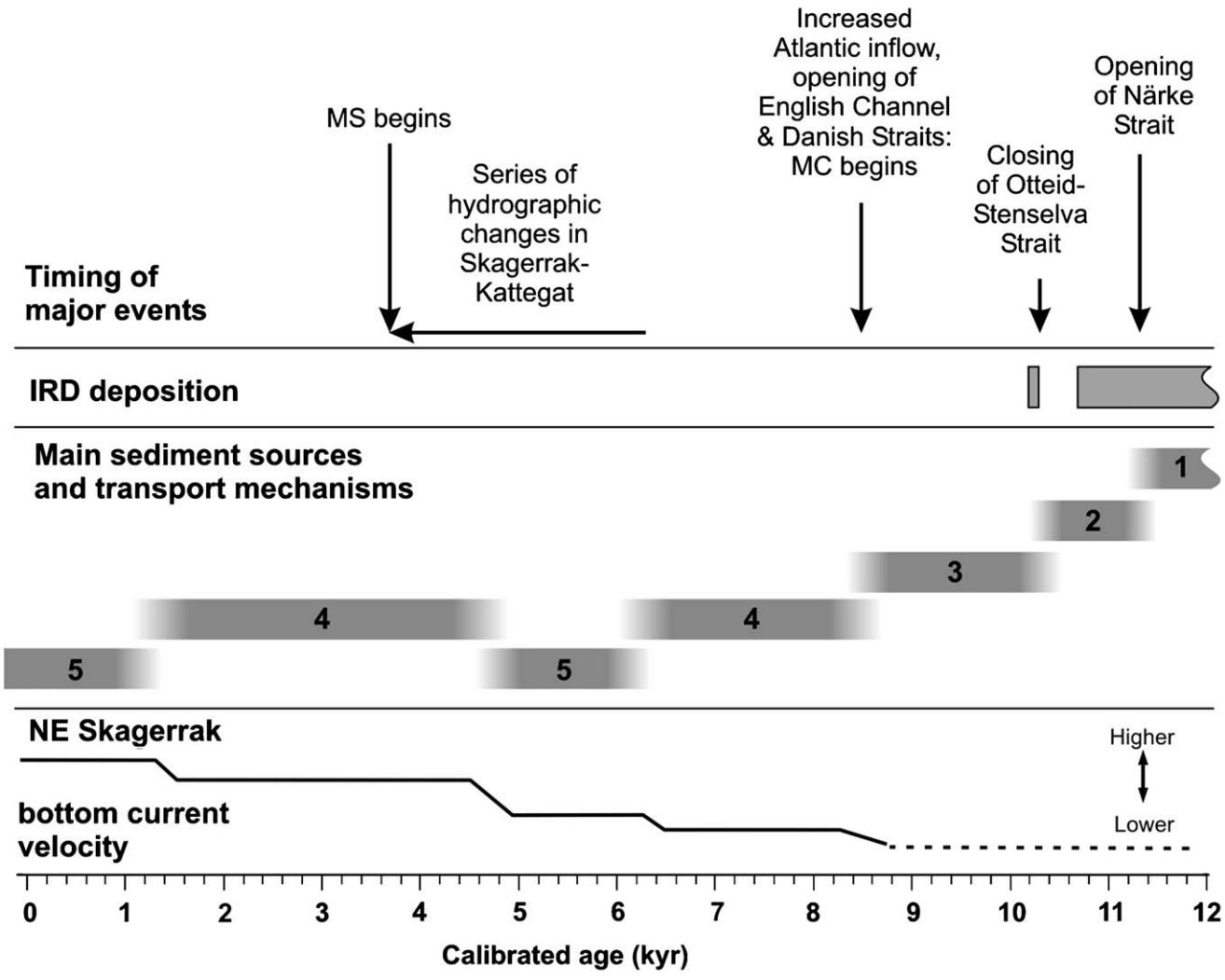

Fig. 9. Schematic compilation of important circulation, sedimentation and provenance changes in the Skagerrak during the Lateglacial and the Holocene. "MC begins": initiation of modern type of circulation in the Skagerrak–Kattegat. "MS begins": development of modern type of sedimentation pattern in the Skagerrak–Kattegat. 1 = glacial marine sediment input through meltwater discharge from southern Norway and SW Sweden; 2 = glacial marine sediment input through meltwater outflow from the Baltic Sea via the Vänern basin; 3 = marine sediment input from the eastern North Sea via the North Jutland Current, 4 and 5 = sediment input chiefly from the southern North Sea and the Atlantic Ocean, transported by the North and South Jutland Current; 4 is distinguished from 5 through sediment input from the Baltic Sea and reworked coastal sediments in Sweden and Norway transported by the Baltic Current and currents along the coasts of western Sweden and southern Norway. The interpreted bottom current velocity is based on the sortable silt median (Fig. 2), and the dashed line indicate an interval where this proxy is less reliable due to low amounts of sortable silt (Fig. 2).

opening of a passageway for meltwater across south-central Sweden at ca 11.3 cal. kyr.

- *Between about* 11.3 *and* 10.3 *cal. kyr*: Sedimentation was dominated by re-deposited glacial sediments from the Baltic Sea and the Vänern Basin, transported by meltwater outflow across south-central Sweden. The sediment transport pattern changed as a result of the closing of the Otteid-Stenselva outlet at ca 10.3 cal. kyr.
- *Between about* 10.3 *and* 8.5 *cal. kyr*: Sedimentation changed from clay-rich distal glacial marine to normal marine sedimentation, governed by the North Jutland Current, with sediments derived predominantly from the eastern North Sea.
- *At about* 8.5 *cal. kyr*: Hydrographic shift occurred as a result of increased Atlantic inflow; former land areas west of Denmark were transgressed; opening of the English Channel and the Danish Straits. This shift marks the initiation of the modern type of circulation in the Skagerrak–Kattegat, with sediments derived predominantly from the Atlantic Ocean and the North Sea, with varying contributions from the South Jutland Current, the Baltic Current, and the currents along the coasts of western Sweden and southern Norway.
- *Between about* 8.2 *and* 6.4 *cal. kyr*: Influence on the sedimentation by the Baltic Current and the currents along the Swedish and Norwegian coasts (''Norwegian'' signature) decreased gradually, while the bottom current strength in the north-eastern Skagerrak increased slightly.
- *Between about* 6.2 *and* 4.7 *cal. kyr*: Baltic outflow and the currents along the Swedish and Norwegian coasts were weaker, and the influence of the Jutland Current increased (more ''Danish'' signature). At ca 4.7 cal. kyr, the bottom current strength increased in the north-eastern Skagerrak, and the provenance started to gradually change to a more ''Norwegian'' signature.
- *Between about* 4.0 *and* 1.5 *cal. kyr*: Influence of the Baltic Current and the currents along the Swedish and Norwegian coasts were higher (''Norwegian'' signature), and the north-eastern Skagerrak bottom current strength was relatively stable.
- *Between about* 1.5 *and* 0.9 *cal. kyr*: Provenance changed clearly to a ''Danish'' signature. The north-eastern Skagerrak bottom current strength increased at ca 1.3 cal. kyr.
- *Between* 0.0 *and* 0.9 *cal. kyr*: Strong but decreasing ''Danish'' signature, and strong but variable bottom current velocities in the north-eastern Skagerrak, strongly influenced by regional climate.

Acknowledgments

Jan Backman and Eve Arnold supervised Richard Gyllencreutz, and are thanked for great support and encouragement through this study, and for their constructive comments on this paper. We are grateful to Thomas Andrén and Svante Björck for fruitful discussions. Hui Jiang kindly provided salinity data. Anders Warén identified the shell material used for 14C-dating. This project was partly funded through Grants from EU-HOLSMEER and the Swedish Research Council to Jan Backman in Sweden, by the French Atomic Energy Commission (CEA) and the Programme National d'Etude de la Dynamique du Climat-IMPAIRS (CNRS). The authors are also grateful to two anonymous reviewers for constructive criticism. This is LSCE contribution 1691.

References

Abrahamsen, N., 1982. Magnetostratigraphy. In: Olausson, E. (Ed.), The Pleistocene/Holocene Boundary in South-Western Sweden. Geological Survey of Sweden, C794, pp. 93–119.

Andersen, B.G., Mangerud, J., Sørensen, R., Reite, A., Sveian, H., Thoresen, M., Bergström, B., 1995. Younger Dryas ice-marginal deposits in Norway. Quaternary International 28, 147–169.

Andrén, T., Lindeberg, G., Andrén, E., 2002. Evidence of the final drainage of the Baltic Ice Lake and the brackish phase of the Yoldia Sea in glacial varves from the Baltic Sea. Boreas 31, 226–238.

Bard, E., Hamelin, B., Fairbanks, R.G., Zindler, A., 1990. Calibration of the ^{14}C timescale over the past 30 000 years using mass spectrometric U-Th ages from Barbados corals. Nature 345, 405–410.

Beierle, B.D., Lamoureux, S.F., Cockburn, J.M.H., Spooner, I., 2002. A new method for visualizing sediment particle size distributions. Journal of Paleolimnology 27, 279–283.

Bennike, O., Jensen, J.B., Lemke, W., Kuijpers, A., Lomholt, S., 2004. Late- and postglacial history of the Great Belt, Denmark. Boreas 33, 18–33.

Berglund, B.E., 1979. The deglaciation of southern Sweden 13,500–10,000 B.P. Boreas 8, 89–118.

Bergsten, H., 1989. Stratigraphy of a Late Weichselian-Holocene Clay Sequence at Göteborg, South-Western Sweden. Department of Geology, Chalmers University of Technology and University of Gothenburg, A 68, pp. 1–115.

Bergsten, H., 1991. Late Weichselian-Holocene Stratigraphy and Environmental Conditions in the Gothenburg Area, South-Western Sweden. Department of Geology, Chalmers University of Technology and University of Gothenburg, A 70, pp. 1–109.

Bergsten, H., 1994. A high-resolution record of Lateglacial and Early Holocene marine sediments from southwestern Sweden; with special emphasis in environmental changes close to the Pleisocene-Holocene transition and the influence of fresh water from the Baltic basin. Journal of Quaternary Science 9, 1–12.

Björck, S., 1995. A review of the history of the Baltic Sea, 13.0–8.0 ka BP. Quaternary International 27, 19–40.

Björck, J., Andrén, T., Wastegård, S., Possnert, G., Schoning, K., 2002. An event stratigraphy for the Last Glacial–Holocene transition in eastern middle Sweden: results from investigations of varved clay and terrestrial sequences. Quaternary Science Reviews 21, 1489–1501.

Björck, S., Koç, N., Skog, G., 2003. Consistently large marine reservoir ages in the Norwegian Sea during the last deglaciation. Quaternary Science Reviews 22, 429–435.

Bøe, R., Thorsnes, T.H. (Eds.), 1996. Marine geology in the Skagerrak and Kattegat. Geological Survey of Norway Bulletin 430, 1–144.

Bøe, R., Rise, L., Thorsnes, T.H., de Haas, H., Saether, O.M., Kunzendorf, H., 1996. Sea-bed sediments and sediment accumulation rates in the Norwegian part of Skagerrak. Geological Survey of Norway Bulletin 430, 75–84.

Bondevik, S., Birks, H.H., Gulliksen, S., Mangerud, J., 1999. Late Weichselian marine ^{14}C reservoir ages at the western coast of Norway. Quaternary Research 52, 104–114.

Brachfeld, S.A., Kissel, C., Laj, C., Mazaud, A., 2004. Behavior of u-channels during acquisition and demagnetization of remanence: implications for paleomagnetic and rock magnetic measurements. Physics of the Earth and Planetary Interiors 145, 1–8.

Colin, C., Kissel, C., Blamart, D., Turpin, L., 1998. Magnetic properties of sediments in the Bay of Bengal and the Andaman Sea: impact of rapid North Atlantic Ocean climatic events on the strength of the Indian monsoon. Earth and Planetary Science Letters 160, 623–635.

Conradsen, K., 1995. Late Younger Dryas to Holocene palaeoenvironments of the southern Kattegat, Scandinavia. The Holocene 5, 447–456.

Conradsen, K., Heier-Nielsen, S., 1995. Holocene paleoceanography and paleoenvironments of the Skagerrak–Kattegatt, Scandinavia. Paleoceanography 10, 810–813.

Day, R., Fuller, M., Schmidt, V.A., 1977. Hysteresis properties of titanomagnetites; grain-size and compositional dependence. Physics of the Earth and Planetary Interiors 13 (4), 260–267.

Eisma, D., Irion, G., 1988. Suspended matter and sediment transport. In: Salomons, W., Bayne, B.L., Duursma, E.K., Förstner, U. (Eds.), Pollution of the North Sea, An Assessment. Springer, Berlin, pp. 20–35.

Eisma, D., Kalf, J., 1987. Dispersal, concentration and deposition of suspended matter in the North Sea. Journal of the Geological Society, London 144, 161–178.

Fält, L.-M., 1982. Late Quaternary sea-floor deposits off the Swedish west coast. Ph.D. Thesis, Chalmers University of Technology and University of Gothenburg, A 37, pp. 1–259.

Gyllencreutz, R., 2005. Late Glacial and Holocene paleoceanography in the Skagerrak from high-resolution grain size records. Palaeogeography, Palaeoclimatology, Palaeoecology 222, 344–369.

Gyllencreutz, R., Jakobsson, M., Backman, J., 2005. Holocene sedimentation in the Skagerrak interpreted from chirp sonar and core data. Journal of Quaternary Science 20, 21–32.

Hafsten, U., 1983. Shore-level changes in South Norway during the last 13,000 years, traced by biostratigraphical methods and radiometric datings. Norsk Geografisk Tidsskrift 37, 63–79.

Hass, H.C., 1996. Northern Europe climate variations during late Holocene: evidence from marine Skagerrak. Palaeogeography, Palaeoclimatology, Palaeoecology 123, 121–145.

Jelgersma, S., 1979. Sea-level changes in the North Sea basin. In: Oerle, E., Shüttenhelm, R.T.E., Wiggers, A.J. (Eds.), The Quaternary History of the North Sea. Symposia Universitatis Upsaliensis Annum Quingentesimum Celebrantis 2, pp. 233–248.

Jiang, H., Björck, S., Knudsen, K.L., 1997. A palaeoclimatic and palaeoceanographic record of the last 11000 ^{14}C years from the Skagerrak–Kattegat, northeastern Atlantic margin. The Holocene 7, 301–310.

Jiang, H., Bjorck, S., Svensson, N.-O., 1998. Reconstruction of Holocene sea-surface salinity in the Skagerrak–Kattegat: a climatic and environmental record of Scandinavia. Journal of Quaternary Science 13, 107–114.

Kissel, C., Laj, C., Labeyrie, L., Dokken, T., Voelker, A., Blamart, D., 1999. Magnetic signature of rapid climatic variations in North Atlantic sediments. In: Abrantes, F., Mix, A.C. (Eds.), Reconstructing Ocean History; A Window into the Future. Kluwer Academic/Plenum Publishers, New York, pp. 419–437.

Klitgaard-Kristensen, D., Sejrup, H.P., Haflidason, H., 2001. The last 18 kyr fluctuations in Norwegian Sea surface conditions and implications for the magnitude of climatic change: evidence from the North Sea. Paleoceanography 5, 455–467.

Knudsen, K.L., Conradsen, K., Heier-Nielsen, S., Seidenkrantz, M.-S., 1996. Quaternary palaeoceanography and palaeogeography in northern Denmark: a review of the results from the Skagen cores. Bulletin of the Geological Society of Denmark 43, 22–31.

Kranck, K., Milligan, T.G., 1991. Grain size in oceanography. In: Syvitski, J.P.M. (Ed.), Principles, Methods and Application of Particle Size Analysis. Cambridge University Press, New York, pp. 332–345.

Kuijpers, A., Dennegård, B., Albinsson, Y., Jensen, A., 1993. Sediment transport pathways in the Skagerrak and Kattegat as indicated by sediment Chernobyl radioactivity and heavy metal concentrations. Marine Geology 111, 231–244.

Lambeck, K., 1995. Late Devensian and Holocene shorelines of the British Isles and North Sea from models of glacio-hydro-isostatic rebound. Journal of the Geological Society, London 152, 437–448.

Lambeck, K., 1999. Shoreline displacements in southern-central Sweden and the evolution of the Baltic Sea since the last maximum glaciation. Journal of the Geological Society, London 156, 465–486.

Lambeck, K., Smither, C., Johnston, P., 1998. Sea-level change, glacial rebound and mantle viscosity for northern Europe. Geophysical Journal International 134, 102–144.

Lepland, A., Stevens, R.L., 1996. Mineral magnetic and textural interpretations of sedimentation in the Skagerrak, eastern North Sea. Marine Geology 135, 51–64.

Le Renard, J., 2005. CLEMAM Check List of European Marine Mollusca, available on the internet at http://www.somali.asso.fr/clemam/index.clemam.html (accessed 06 September 2005).

Leth, J.O., 1996. Late Quaternary geological development of the Jutland Bank and the initiation of the Jutland Current, NE North Sea. Geological Survey of Norway Bulletin 430, 25–34.

Liebezeit, G., van Weering, T.C.E., Rumohr, J. (Eds.), 1993. Special issue: Holocene sedimentation in the Skagerrak. Marine Geology 111, 189–379.

Longva, O., Thorsnes, T. (Eds.), 1997. Skagerrak in the past and present—an integrated study of geology, chemistry, hydrography and microfossil ecology. NGU Special Publication 8, 1–100.

Lundqvist, J., Wohlfarth, B., 2001. Timing and east-west correlation of south Swedish ice marginal lines during the Late Weichselian. Quaternary Science Reviews 20, 1127–1148.

McCave, I.N., Manighetti, B., Robinson, S.G., 1995. Sortable silt and fine sediment size/composition slicing: parameters for paleocurrent speed and paleoceanography. Paleoceanography 10, 593–610.

Mörner, N.-A., 1979. The deglaciation of Sweden: a multi-parameter consideration. Boreas 8, 189–198.

Nordberg, K., 1991. Oceanography in the Kattegat and Skagerrak over the past 8000 years. Paleoceanography 4, 461–484.

Nordberg, K., Bergsten, H., 1988. Biostratigraphic and sedimentological evidence of hydrographic changes in the Kattegat during the later part of the Holocene. Marine Geology 83, 135–158.

Olsen, L., Sveian, H., Berstrøm, B., 2001. Rapid adjustments of the western part of the Scandinavian Ice Sheet during the mid and late Weichselian—a new model. Norsk Geologisk Tidsskrift 81, 93–118.

Otto, L., Zimmerman, T.F., Furnes, G.K., Mork, M., Saetre, R., Becker, G., 1990. Review of the physical oceanography of the North Sea. Netherlands Journal of Sea Research 26, 161–238.

Pederstad, K., Roaldset, E., Rønningsland, T.M., 1993. Sedimentation and environmental conditions in the inner Skagerrak—outer Oslofjord. Marine Geology 111, 245–268.

Petersen, K.S., 2004. Late Quaternary environmental changes recorded in the Danish marine molluscan faunas. Geological Survey of Denmark and Greenland Bulletin 3, 258–259.

Robinson, S.G., Maslin, M.A., McCave, I.N., 1995. Magnetic susceptibility variations in Upper Pleistocene deep-sea sediments of the NE Atlantic: implications for ice rafting and palaeocirculation at the last glacial maximum. Paleoceanography 10, 221–250.

Rodhe, J., 1987. The large-scale circulation in the Skagerrak; interpretation of some observations. Tellus 39A, 245–253.

Rodhe, J., 1996. On the dynamics of the large-scale circulation of the Skagerrak. Journal of Sea Research 35, 9–21.

Rodhe, J., 1998. The Baltic and North Seas: a process-oriented review of the physical oceanography. In: Robinson, A.R., Brink, K.H. (Eds.), The Sea, vol. 11. Wiley, New York, pp. 699–732.

Rodhe, J., Holt, N., 1996. Observations of the transport of suspended matter into the Skagerrak along the western and northern coast of Jutland. Journal of Sea Research 35, 91–98.

Schoenharting, G., 1985. Magnetostratigraphy and rock magnetic properties of the sediment core GIK 15530-4 from the Skagerrak. Norsk Geologisk Tidsskrift 65, 37–40.

Smith, W.H.F., Sandwell, D.T., 1997. Global sea floor topography from satellite altimetry and ship depth soundings. Science 5334, 1956–1962.

Snowball, I.F., 1991. Magnetic hysteresis properties of greigite (Fe_3S_4) and a new occurrence in Holocene sediments from Swedish Lappland. Physics of the Earth and Planetary Interiors 68, 32–40.

Sørensen, R., 1979. Late Weichselian deglaciation in the Oslofjord area, south Norway. Boreas 8, 241–246.

Sørensen, R., 1992. The physical environment of Late Weichselian deglaciation of the Olsofjord region, southeastern Norway. Geological Survey of Sweden Ca 81, 339–346.

Stabell, B., Thiede, J. (Eds.), 1985. Upper Quaternary marine Skagerrak (NE North Sea) deposits: stratigraphy and depositional environment. Norsk Geologisk Tidsskrift 65, 1–149.

Stabell, B., Thiede, J., 1986. Paleobathymetry and paleogeography of southern Scandinavia in the late Quaternary. Meyniana 38, 43–59.

Stuiver, M., Reimer, P.J., 1993. Extended ^{14}C data base and revised CALIB 3.0 ^{14}C age calibration program. Radiocarbon 35, 215–230.

Stuiver, M., Reimer, P.J., Braziunas, T.F., 1998. High-precision radiocarbon age calibration for terrestrial and marine samples. Radiocarbon 40, 1127–1151.

Svansson, A., 1975. Physical and chemical oceanography of the Skagerrak and Kattegat. I. Open sea conditions. Fishery Board of Sweden, Institute of Marine Research Report 1, 1–88.

Tauxe, L., LaBrecque, J.L., Dodson, R., Fuller, M., DeMatteo, J., 1983. "U" channels; a new technique for paleomagnetic analysis of hydraulic piston cores. Eos, Transactions, American Geophysical Union 18, 219 (abstract).

Telford, R.J., Heegard, E., Birks, H.J.B., 2004. The intercept is a poorly behaved estimate of a calibrated radiocarbon age. The Holocene 14, 296–298.

Thiede, J., 1987. The late Quaternary Skagerrak and its depositional environment. Boreas 16, 425–432.

van Weering, T.C.E., 1981. Recent sediments and sediment transport in the northern North Sea; surface sediments of the Skagerrak. In: Nio, S.-D., Schüttenhelm, R.T.E., van Weering, T.C.E. (Eds.), Holocene Marine Sedimentation in the North Sea Basin, vol. 5. Special Publication of the International Association of Sedimentologists, pp. 335–359.

van Weering, T.C.E., 1982. Recent sediments and sediment transport in the northern North Sea; pistoncores from the Skagerrak. Proceedings of the Koninklijke Nederlandse Akademie van Wetenschappen B 85, pp. 155–201.

van Weering, T.C.E., Berger, G.W., Okkels, E., 1993. Sediment transport, resuspension and accumulation rates in the northeastern Skagerrak. Marine Geology 111, 269–285.

Weeks, R., Laj, C., Endignoux, L., Fuller, M., Roberts, A., Manganne, R., Blanchard, E., Goree, W., 1993. Improvements in long-core measurement techniques; applications in palaeomagnetism and palaeoceanography. Geophysical Journal International 114, 651–662.